Flat plate self-noise reduction at low-to-moderate Reynolds number with trailing edge serrations

Danielle J. Moreau, Laura A. Brooks and Con J. Doolan

School of Mechanical Engineering, The University of Adelaide, Adelaide, South Australia, 5005, Australia

ABSTRACT

This paper explores the noise reduction potential of sawtooth trailing edge serrations on a flat plate at low-to-moderate Reynolds number. The noise radiated by a flat plate with both sharp and serrated trailing edges has been measured in an anechoic wind tunnel at the University of Adelaide. The noise measurements have been taken at a range of flow speeds (Reynolds numbers of $Re_c < 4.5 \times 10^5$, based on chord) for two different sawtooth geometries. Trailing edge serrations are found to achieve an average attenuation of up to 7 dB over a certain Strouhal number range, where Strouhal number is $St = f\delta/U_\infty$, f is frequency, δ is boundary layer thickness and U_∞ is the free stream velocity. The results of this study are compared with theoretical noise reduction predictions showing that significant differences exist between measurements and theory.

INTRODUCTION

Trailing edge noise is produced by the scattering of boundary layer turbulence at an airfoil trailing edge, resulting in radiation of broadband acoustic energy. A tonal noise component may also be produced when vortices are shed from the trailing edge. Trailing edge noise is considered to be the dominant noise source in many applications that use airfoil shapes such as aircraft, submarines and wind turbines (Blake 1986, Lockard and Lilley 2004, Oerlemans et al. 2009). The reduction of trailing edge noise is a subject of much interest due to its practical relevance to a wide range of applications. Trailing edge serrations have been shown both theoretically (Howe 1991a; 1991b) and experimentally (Dassen et al. 1996, Braun et al. 1999, Parchen et al. 1999, Oerlemans et al. 2001; 2009, Gruber et al. 2010; 2011) to produce significant reductions in the trailing edge noise radiated into the far-field.

According to Howe (1998), the far-field acoustic pressure spectrum of a flat plate airfoil, $\Phi(\mathbf{x},\omega)$, at an observer location a distance $|\mathbf{x}|$ from the trailing edge can be approximated as

$$\Phi(\mathbf{x},\omega) \approx \frac{M_c L \sin^2\left(\frac{\theta}{2}\right)\sin(\alpha)}{2\pi^2|\mathbf{x}|^2} l_2 \psi(\omega), \qquad (1)$$

where M_c is the convection Mach number, l_2 is the spanwise correlation length scale of turbulence near the trailing edge, L is the length of the trailing edge wetted by the turbulent flow, θ and α are the polar and azimuthal observer angles respectively, $\psi(\omega)$ is the turbulent surface pressure spectrum close to the trailing edge and $\omega = 2\pi f$, where f is the frequency. The polar and azimuthal observer angles, θ and α, are defined according to the co-ordinate system shown in Fig. 1. The convection Mach number is defined as $M_c = U_c/c_0$, where U_c is the convection speed of the principal turbulence eddies and c_0 is the speed of sound.

Howe (1991a; 1991b) assumes that the turbulent surface pressure spectrum, $\psi(\omega)$, is unaffected by the presence of the trailing edge serrations. Therefore, according to Eq. (1), for a given observer location the trailing edge noise can be reduced by minimising either the spanwise correlation length scale, l_2, or the length of the wetted surface, L. Trailing edge serrations are believed to reduce the radiated noise by minimising the effective spanwise length of the trailing edge that contributes to noise generation. This is even though serrations increase the physical length of the trailing edge (Howe, 1991a).

Howe (1991a; 1991b) conducted a theoretical investigation on the noise produced by low Mach number flow over the trailing edge of a flat plate with serrations at zero angle of attack. Consider a serrated trailing edge to have a root to tip amplitude of $2h$ and wavelength of λ, as shown in Fig. 2. Howe (1991a; 1991b) showed that when the acoustic frequency is high such that $\omega h/U_\infty >> 1$, the theoretical maximum noise reduction in radiated mean square pressure is proportional to $6h/\lambda$ for sinusoidal serrations and $10\log_{10}[1+(4h/\lambda)^2]$ for serrations with a sawtooth profile. The largest noise reductions occur when the dimensions of the serrations are at minimum the order of the turbulent boundary layer thickness and when the angle between the mean flow and the local tangent to the wetted surface is less than 45°. This suggests that sharper serrations will result in greater noise reduction. According to Howe (1991a; 1991b), sound generated by large eddies whose length scales are greater than the amplitude of the serrations (low frequency sound) is unaffected by the presence of the serrations. Significant noise reductions can only be expected in the high frequency region when $\omega h/U_\infty >> 1$.

The majority of experimental studies on trailing edge serrations have been conducted on full scale wind turbine blades or wind tunnel scale airfoil models at high Reynolds numbers ($Re_c > 5 \times 10^5$) (Braun et al. 1999, Parchen et al. 1999, Oerlemans et al. 2001; 2009, Gruber et al. 2010; 2011). Oerlemans et al. (2001) investigated the reduction of trailing edge noise from a NACA 64418 airfoil at a high Reynolds number of $Re_c \approx 1.6 \times 10^6$ by shape optimisation and the application of trailing edge serrations. Optimising the airfoil shape for low noise emission achieved ~4 dB of attenuation in the radiated noise levels over a variety of flow conditions. An additional 2 dB of attenuation was achieved by adding trailing

edge serrations. Oerlemans et al. (2009) later investigated airfoil shape optimisation and trailing edge serrations for a full scale wind turbine. The General Electric 2.3 MW wind turbine used in experiments had a diameter of 94 m and three blades. The trailing edge serrations were found to decrease noise levels at frequencies below 1 kHz and increase the noise levels above this frequency without any adverse effect on aerodynamic performance. The high frequency noise increase was attributed to misalignment of the serrations with flow direction. The overall noise reductions obtained with the optimised airfoil and trailing edge serrations were 0.5 dB and 3.2 dB respectively.

As part of the European project FLOCON (Adaptive and Passive Flow Control for Fan Broadband Noise Reduction), Gruber et al. (2010; 2011) investigated the airfoil self-noise reduction achieved with sawtooth serrations on a NACA651-210 airfoil at $Re_c < 8.5 \times 10^5$. Contrary to Howe's predictions, the largest noise reductions (up to 7 dB) were achieved at low to mid frequencies (< 2 kHz) and an increase in noise level was observed at high frequencies (> 7 kHz) with trailing edge serrations. Theoretical noise predictions obtained with Howe's (1991b) theory were found to differ significantly from noise measurements by up to 30 dB. The measured noise reductions achieved with trailing edge serrations displayed a linear dependence on Strouhal number with the noise level increasing above a critical frequency, f_0, corresponding to $St_0 = f_0\delta/U_\infty \sim 1$, where δ is the boundary layer thickness and U_∞ is the free stream velocity.

To the authors' knowledge, Dassen et al. (1996) are the only researchers to have experimentally examined the effect of trailing edge serrations on flat plate models. They conducted wind tunnel tests on a series of flat plates and NACA airfoils both with and without serrations at high Reynolds numbers of $7 \times 10^5 < Re_c < 1.4 \times 10^6$. Serrations applied to the flat plates produced > 5dB reduction in the radiated noise levels over 1 - 6 kHz. This is less than the attenuation predicted with the theory of Howe (1991b).

While most of the studies on the trailing edge serrations have focused on turbulent boundary layer broadband noise at high Reynolds numbers, Chong et al. (2010; 2011) were one of the few to investigate their capability in reducing airfoil instability noise at low-to-moderate Reynolds numbers. In this study, acoustic tests were conducted on a NACA 0012 airfoil at various angles of attack and Reynolds numbers of $1 \times 10^5 < Re_c < 5 \times 10^5$. In this Reynolds number range, the airfoil self-noise spectra contained a broadband contribution and a number of high amplitude tonal components. Trailing edge serrations were found to inhibit flow separation close to the trailing edge and in turn reduce the amplitude of the broadband and tonal noise components. Contrary to the findings of Howe (1991b), larger reductions in the tonal noise components were achieved with large serration angles between the mean flow and the local tangent to the wetted surface.

All experimental studies conducted on trailing edge serrations in the past have reported some discrepancy between Howe's (1991b) theory and measurements. In all cases, the predicted noise reduction levels far exceeded those measured. In addition, contrary to Howe's (1991b) theory, trailing edge serrations on airfoils have been found to produce a noise reduction at low frequencies and a noise increase at high frequencies (Braun et al. 1999, Parchen et al., 1999, Gruber et al., 2010; 2011).

This paper presents results of an experimental study on the noise reduction potential of sawtooth trailing edge serrations on a flat plate at low-to-moderate Reynolds number ($Re_c < 4.5 \times 10^5$).The aims of this paper are (1) to present acoustic data for two different serrations geometries at a variety of flow speeds and (2) to compare experimental measurements with noise reductions predicted using the theory of Howe (1991a; 1991b). The results presented in this paper are the preliminary results of a much larger study to gain insight into the serration noise reduction mechanism for quiet airfoil development.

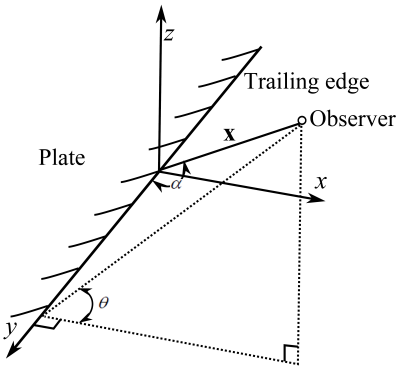

Figure 1. Flat plate co-ordinate system.

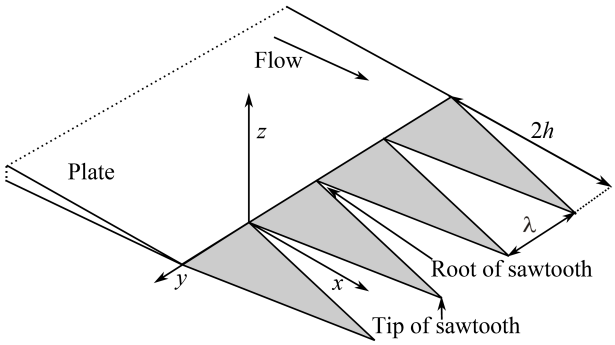

Figure 2. Sawtooth serrations at the trailing edge of a flat plate with root-to-tip amplitude of 2h and wavelength of λ.

EXPERIMENTAL METHOD

Testing was conducted in the anechoic wind tunnel at the University of Adelaide. The anechoic wind tunnel test chamber is 1.4 m × 1.4 m × 1.6 m (internal dimensions) and has walls that are acoustically treated with foam wedges to provide a reflection free environment (ideally) above 200 Hz. The facility contains a rectangular contraction with a height of 75 mm and a width of 275 mm. The maximum flow velocity of the free jet is ~40 m/s and the free-stream turbulence intensity is low at 0.3% (Moreau et al., 2010a).

The flat plate model used in this study is composed of a main steel body and a detachable trailing edge plate made from brushed aluminium, as shown in Fig. 3. The main body has a span of 450 mm and a thickness of 5 mm. The leading edge (LE) of the main body is elliptical with a semi-major axis of 8 mm and a semi-minor axis of 2.5 mm while the trailing edge (TE) is asymmetrically beveled at an angle of 12°. Three 0.5 mm thick trailing edge plates were used (one at a time) as shown in Fig. 4 (a): one with a straight, unserrated

configuration and two with serrations. The flat plate model with the straight unserrated trailing edge is used as the reference configuration for all tests and so will be referred to as the reference plate hereafter. Two different serration geometries are compared in this study: one with a wavelength of λ= 3 mm (termed narrow serrations) and the other with λ= 9 mm (termed wide serrations). Both serrations had root-to-tip amplitude of 2h = 30 mm. As shown in Fig. 4 (b), the root of the serrations is aligned with the trailing edge of the main body so that only the serrated component of the trailing edge plate is exposed to the flow. The area of the reference plate is equivalent to that of the flat plates with serrated trailing edges giving the same effective wetted surface area in all three test cases. The serrated and reference plate models all have the same mean chord of 165 mm.

The trailing edge plate is fastened to the main body with 24 M2 x 0.4 screws. These screws protruded slightly into the flow below the lower flat surface of the plate model; however this was consistent for all three plate configurations. The method of trailing edge attachment used in this study avoids bluntness at the root of the serrations that may produce vortex shedding and a tonal noise component. The flat plate model was then held between two side plates and attached to the contraction at zero angle of attack as shown in Fig. 4 (b). The span of the flat plate models extends beyond the width of the contraction outlet (see Fig. 4 (b)) to eliminate the noise produced by the interaction of the side plate boundary layers with the model leading edge.

The acoustic measurements were recorded at a single observer location using a B&K 1/2" microphone (Model No. 4190) located 554 mm directly below the trailing edge of the reference plate. Experiments were conducted at various flow speeds between U_∞ = 7 and 38 m/s. At each selected flow speed, noise data were recorded using a National Instruments board at a sampling frequency of 5 × 10^4 Hz for a sample time of 8 s.

EXPERIMENTAL RESULTS AND DISCUSSION

Acoustic measurements for the reference plate

The far-field acoustic spectra for the reference plate with a straight trailing edge at free-stream velocities between U_∞ = 7 and 38 m/s are shown in Fig. 5. The acoustic spectra measured at speeds between U_∞ = 15 and 38 m/s follow a clear trend with noise levels decreasing for a reduction in flow velocity (see Fig. 5 (a)). This is particularly evident at lower frequencies (< 1 kHz) where high noise levels are measured. Additionally, the broad hump observed at high frequencies (at 9.5 kHz for U_∞ = 38 m/s) reduces in frequency and amplitude with decreasing flow speed.

Figure 5 (b) shows that below U_∞ = 12 m/s, the noise spectra do not follow the trends observed at higher flow speeds in Fig. 5 (a). At flow speeds below U_∞ = 12 m/s, the noise levels at low frequencies are observed to increase in amplitude with decreasing flow speed, reach a peak at 9 m/s and then reduce in amplitude with a further reduction in flow speed. At these low flow velocities, the flat plate boundary layer is expected to be less turbulent than at higher flow speeds and in a more transitional flow state at the trailing edge. The high levels of low frequency noise measured at low flow speeds in Fig. 5 (b) are likely due to eddies or flow perturbations in the transitional boundary layer at the trailing edge.

The noise spectra at speeds below U_∞ = 12 m/s vary with flow velocity and frequency in a very different manner to those at higher flow speeds between U_∞ = 15 and 38 m/s (see Fig. 5). The acoustic behaviour of the flat plate model can therefore be grouped into two regimes: Regime I between U_∞ = 15 and 38 m/s and regime II at U_∞ < 12 m/s.

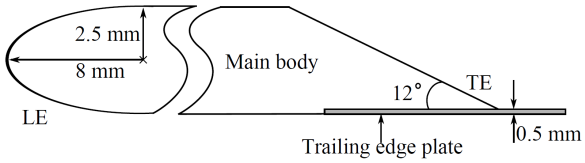

Figure 3. Schematic diagram of the flat plate model.

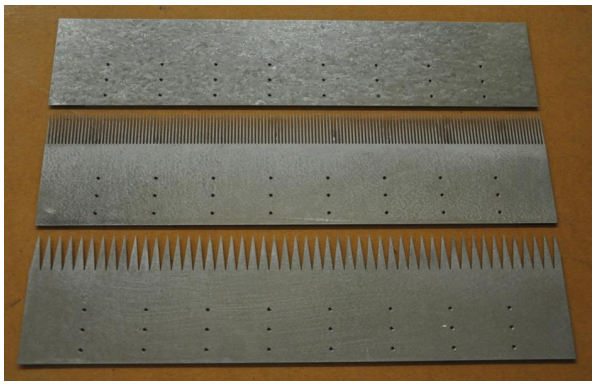

(a) Trailing edge plates. Top: straight unserrated trailing edge, middle: narrow serrations with λ= 3 mm, bottom: wide serrations with λ= 9 mm.

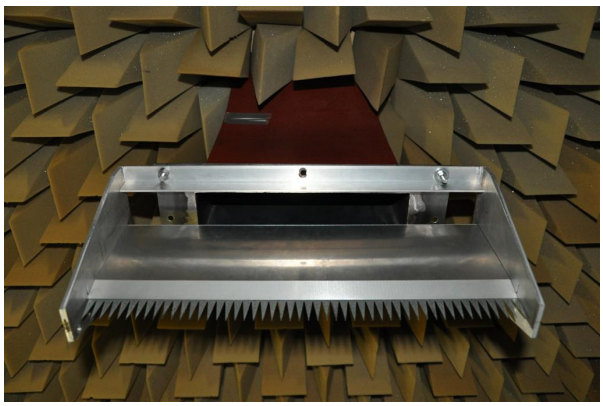

(b) The flat plate model with wide trailing edge serrations held between the side plates and attached to the contraction outlet.

Figure 4. The trailing edge plates and the flat plate model in situ.

Noise reduction with trailing edge serrations

Figures 6 and 7 show the far field acoustic spectra for the reference plate and the two plates with trailing edge serrations at selected free stream velocities in regime I and regime II, respectively. The background noise spectra are also shown in these figures for comparison. Figures 8 and 9 show 2D surface plots of the measured attenuation achieved with the trailing edge serrations in regime I and regime II, respec-

tively. The attenuation in Figs. 8 and 9 has been calculated by dividing the power spectral density of the serrated plates by that of the reference plate. Figure 8 shows the attenuation achieved above U_∞ = 15 m/s in increments of 5m/s while Fig. 9 shows the attenuation achieved below U_∞ = 12 m/s in increments of 1 m/s.

At U_∞ = 38 m/s in regime I, Fig. 6 (a) shows that the noise levels for all three plates are approximately equal at frequencies below 5 kHz. Above this frequency, trailing edge serrations produce a region of noise attenuation. In regime I, this high frequency region of noise attenuation reduces in frequency and amplitude with decreasing flow speed to U_∞ = 15 m/s (see Fig 6 (b)). This trend can be clearly seen in Fig. 8. This figure also shows that in regime I, the two serration configurations perform similarly, with the wide serrations achieving just slightly higher levels of noise attenuation than the narrow ones.

Below U_∞ = 12 m/s in regime II, the wide serrations produce a low frequency region of attenuation (up to ~2 kHz) that increases in amplitude with decreasing flow speed (see Figs. 7 (a) and (b)). This is clearly evidenced by the 2D attenuation map in Fig. 9 (a).

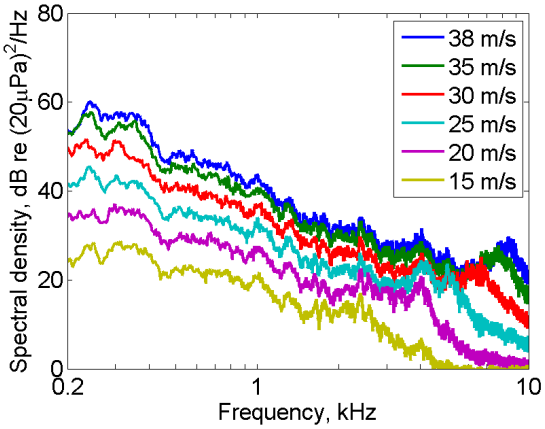

(a) Regime I: U_∞ = 15 – 38 m/s.

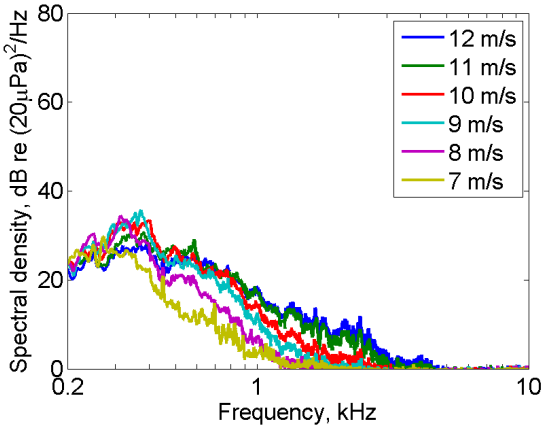

(b) Regime II: U_∞ = 7 – 12 m/s.

Figure 5. Far-field acoustic spectra for the reference plate with a straight trailing edge.

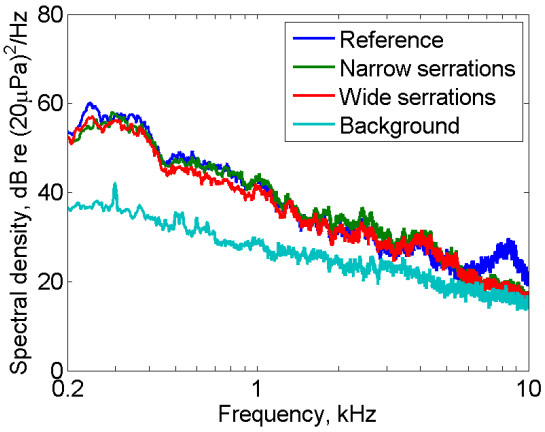

(a) U_∞ = 38 m/s.

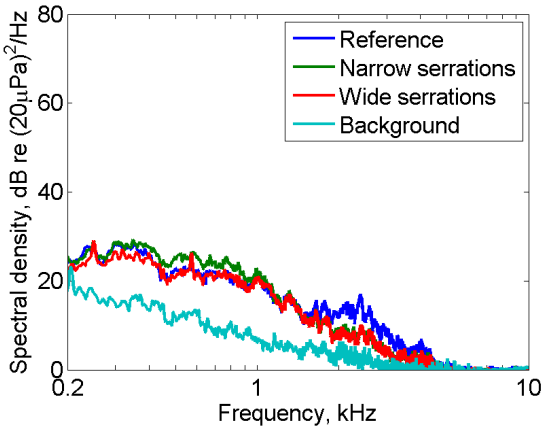

(b) U_∞ = 15 m/s.

Figure 6. Far field acoustic spectra for the reference plate and the plates with trailing edge serrations for two flow velocities in regime I compared to background noise levels.

At U_∞ = 9 m/s in Fig. 7 (b), two peaks are observed in the spectra for the wide serrations. These peaks at 250 and 450 Hz are due to noise produced by the fan in the anechoic wind tunnel facility and are thus not further considered here.

In regime II, between U_∞ = 9 and 12 m/s, a noise increase is produced at low frequencies with the narrow serrations and a number of broad, high amplitude peaks are present in the noise spectra (see Figs. 7 and 9 (b)). These peaks are likely due to vortex shedding from the narrow serrations at the plate trailing edge. Above the peak frequencies, the narrow serrations achieve similar levels of attenuation to the wide serrations. Below flow speeds of U_∞ = 9 m/s, the narrow serrations perform similarly to the wide ones at all frequencies considered in this investigation.

The 2D surface plots of the attenuation achieved with serrations in Fig. 9 show that in regime II, the wide serrations once again outperform the narrow serrations. The wide serrations are observed to produce higher levels of attenuation over a larger frequency range at all flow speeds between U_∞ = 7 and 12 m/s.

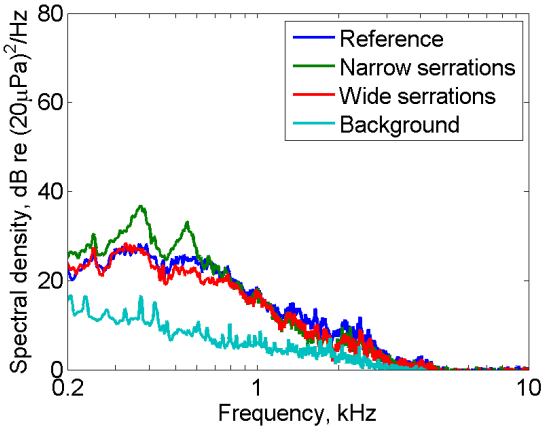

(a) U_∞ = 12 m/s

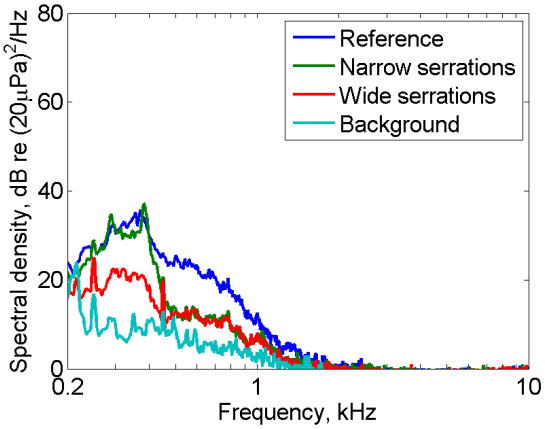

(b) U_∞ = 9 m/s

Figure 7. Far field acoustic spectra for the reference plate and the plates with trailing edge serrations for two flow velocities in regime II compared to background noise levels.

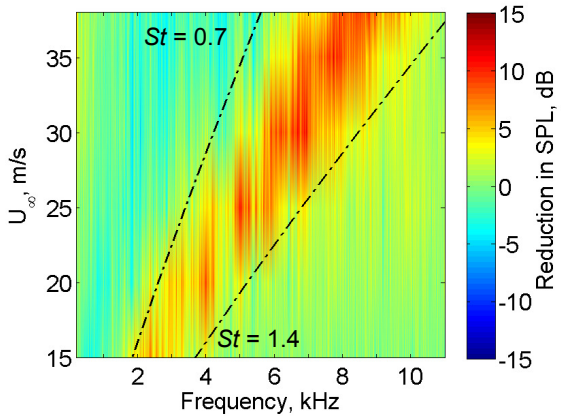

(a) Narrow serrations with λ = 3 mm.

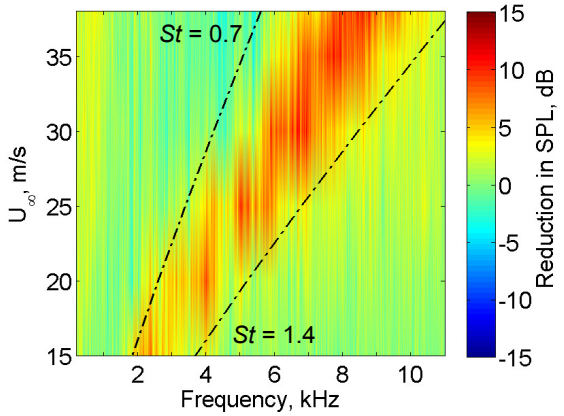

(b) Wide serrations with λ = 9 mm.

Figure 8. Noise reduction achieved with serrations in Regime I at U_∞ = 15 – 38 m/s.

The average attenuation achieved with trailing edge serrations in regimes I and II is given in Table 1. Also tabulated is the frequency range over which this attenuation occurs. This table shows that in regime I, the average noise reduction decreases with a reduction in flow speed. Conversely in regime II, an increase in noise attenuation is observed for a decrease in flow speed. The maximum average attenuation achieved with serrations is 7.3 and 6.9 dB for the wide and narrow serrations respectively. This table confirms that larger noise reductions are produced with the wider serrations than with the narrow ones.

Variation in noise reduction with Strouhal number

The noise attenuation achieved with trailing edge serrations in Figs. 8 and 9 is found to occur over a certain Strouhal number range, where Strouhal number is $St = f\delta/U_\infty$. While the boundary layer thickness, δ, was not directly measured in experiments, it can be approximated using the expression for a turbulent boundary layer on a flat plate as follows (Cebeci and Bradshaw, 1977)

$$\frac{\delta}{c} = \frac{0.37}{Re_c^{1/5}}, \qquad (2)$$

where c is the plate chord. In regime I, Fig. 8 shows that for both trailing edge serration geometries, attenuation is achieved between St = 0.7 and St = 1.4. It is worth noting that this attenuation region is defined by Strouhal numbers based on convective velocity, $St_c = f\delta/U_c$, of $St_c \approx 1$ and $St_c \approx 2$, where $U_c \approx 0.7U_\infty$.

In regime II, Fig. 9 shows that for both trailing edge serration geometries, the major region of noise attenuation is below St = 0.7 ($St_c \approx 1$) with minimal attenuation being achieved between St = 0.7 ($St_c \approx 1$) and St = 1.4 ($St_c \approx 2$).

In their experiments on trailing edge serrations, Gruber et al. (2011) found that the frequency delimiting a noise reduction and a noise increase followed a constant Strouhal number dependency of $St \approx 1$. This Strouhal number scaling does not describe the trends observed in the flat plate data in Figs. 8 and 9. With the exception of the narrow serrations at flow speeds between U_∞ = 9 and 12 m/s, no major noise increase is observed to occur with the addition of trailing edge serrations in this study. Discrepancies in the Strouhal number scaling is attributed to significant differences in Reynolds number and between the geometry of the NACA651-210 airfoil used by Gruber et al. (2011) and the flat plate studied here.

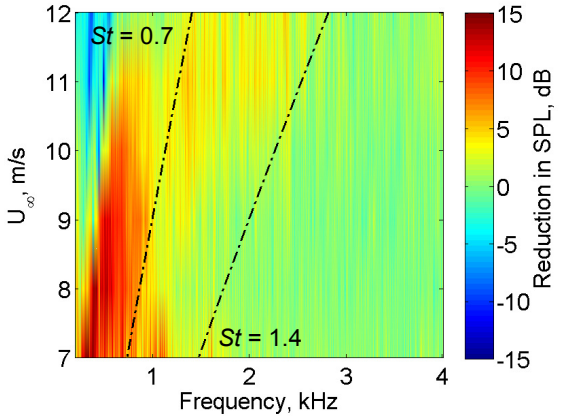

(a) Narrow serrations with λ = 3 mm.

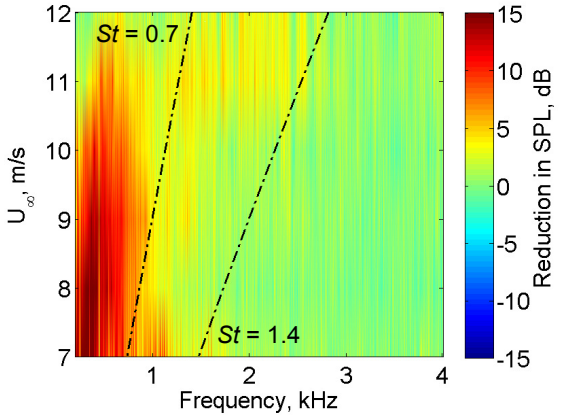

(b) Wide serrations with λ = 9 mm.

Figure 9. Noise reduction achieved with serrations in Regime II at U_∞ = 7 – 12 m/s.

Comparison with serrations theory

According to Howe (1991b), the acoustic pressure frequency spectrum of a flat plate with a serrated trailing edge is given by

$$\frac{\Phi(\mathbf{x},\omega)}{\left(\rho v_*^2\right)^2 (l/c_0)(\delta/|\mathbf{x}|)^2} = \left(\frac{C_m}{\pi}\right)\sin^2\left(\frac{\theta}{2}\right)\sin(\alpha)\Psi(\omega), \qquad (3)$$

where ρ is the fluid density, $v_* \approx 0.03U_\infty$, l is the plate span, c_0 is the speed of sound, $C_m \approx 0.1553$, $\Psi(\omega)$ is the non-dimensional edge noise spectrum and all other parameters are as defined for Eq. (1). Note that the non-dimensional edge noise spectrum, $\Psi(\omega)$, is different from the surface pressure spectrum close to the trailing edge, $\psi(\omega)$, in Eq. (1), which is unaffected by the presence of the trailing edge serrations.

For a serrated trailing edge, the non-dimensional edge noise spectrum is defined as

$$\Psi(\omega) = \left(1+\frac{1}{2}\varepsilon\frac{\partial}{\partial\varepsilon}\right) f\left(\frac{\omega\delta}{U_c}, \frac{h}{\lambda}, \frac{h}{\delta}; \varepsilon\right), \qquad (4)$$

Table 1. Average attenuation achieved with trailing edge serrations.

U_∞, m/s	Frequency range of noise attenuation, Hz		Average attenuation, dB/Hz	
	Narrow serrations	Wide serrations	Narrow serrations	Wide serrations
Regime I				
38	6800 – 9955	6800 - 9955	6.4	6.9
35	5865 - 9080	5865 - 9080	6.4	6.7
30	5615 - 7955	5615 - 7955	6.9	7.0
25	4865 - 6080	4865 - 6080	6.5	6.7
20	2370- 4300	2370- 4300	4.6	4.9
15	1590 - 3430	1590 - 3430	4.1	4.2
Regime II				
12	1160 - 2560	390 - 2560	2.7	2.2
11	560 - 2410	220 - 2410	3.5	3.7
10	500 - 1790	200 - 1790	4.2	4.6
9	325 - 1645	200 - 1645	4.9	6.4
8	220 - 1630	200 - 1630	5.3	6.4
7	200 - 1630	200 - 1630	6.3	7.3

$$f\left(\frac{\omega\delta}{U_c}, \frac{h}{\lambda}, \frac{h}{\delta}; \varepsilon\right) = \frac{1}{(AB+\varepsilon^2)}$$

$$\times\left(1+\frac{64(h/\lambda)^3(\delta/h)A\left(\cosh\left(C\sqrt{A+\varepsilon^2}\right)-\cos(2\omega h/U_c)\right)}{\left(\sqrt{A+\varepsilon^2}\right)(AB+\varepsilon^2)\sinh\left(C\sqrt{A+\varepsilon^2}\right)}\right), \qquad (5)$$

where $A = (\omega\delta/U_c)^2$, $B = 1+(4h/\lambda)^2$, $C = \lambda/2\delta$ and $\varepsilon \approx 1.33$. For the case when $h \to 0$, Eqs. (4) and (5) reduce to the following non-dimensional edge noise spectrum for an unserrated trailing edge

$$\Psi(\omega) = \frac{A}{\left[A+\varepsilon^2\right]^2}. \qquad (6)$$

Figure 10 shows 2D surface plots of the noise reduction predicted with Howe's (1991b) theory for the two different serration geometries used in this study. The predicted attenuation in Fig. 10 has been calculated by dividing the edge spectra of the serrated plates (Eqs. (4) and (5)) with that of the reference plate (Eq. (6)). The oscillations in the theoretical noise reduction map for narrow serrations in Fig. 10 (a) are due to interference between acoustic radiation produced at the root and the tip of the serrations.

The experimental measurements in Figs. 8 and 9 do not agree with Howe's theory in terms of absolute noise levels or in terms of the variation in noise reduction with flow velocity and frequency. Compared with measured attenuation levels,

the theoretical noise reduction predictions are much higher and occur over a much larger frequency range at all flow velocities considered in this study.

According to Howe (1991b), the serration geometry determines the magnitude of the noise reduction. The theoretical maximum attenuation in the radiated mean square pressure is $10\log_{10}(1+(4h/\lambda)^2)$ for serrations with a sawtooth profile. The noise reduction is therefore expected to increase as λ/h decreases. For the narrow serrations with λ = 3 mm, the maximum attenuation is predicted to be 26 dB while for the wide serrations with λ = 9 mm, the maximum theoretical attenuation is 17 dB. As shown in Fig. 10, narrow serrations are predicted to clearly outperform wide serrations in terms of the level of attenuation achieved at all frequencies and flow speeds. In this study however, wide serrations were found to achieve larger attenuation levels than narrow serrations (see Figs. 8 and 9 and Table 1). While contrary to the findings of Howe (1991b), this does agree with the experimental findings of Chong et al. (2010; 2011).

In deriving the serration noise reduction model, Howe (1991b) made numerous assumptions and approximations. One such assumption is that the surface pressure frequency spectrum close to the trailing edge is unchanged by the presence of trailing edge serrations. A number of experimental studies have however, shown that this assumption is inaccurate (Parchen et al. 1999, Gruber et al, 2010). This may explain the considerable over-prediction of noise reduction observed in this and many other experimental studies (Braun et al. 1999, Parchen et al., 1999, Gruber et al., 2010; 2011).

CONCLUSIONS AND FUTURE WORK

This paper has presented the results of an experimental investigation on the noise reduction achieved with trailing edge serrations on a flat plate model at low-to-moderate Reynolds number. Trailing edge serrations were found to achieve a peak attenuation of 14 dB at certain frequencies and up to an average attenuation of 7 dB over a large frequency range at $Re_c < 4.5 \times 10^5$. The measured noise reductions were found to occur over a certain Strouhal number range, with attenuation being achieved between St = 0.7 and St = 1.4 at high flow speeds ($1.7 \times 10^5 < Re_c < 4.5 \times 10^5$) and at $St < 0.7$ at low flow speeds ($Re_c < 1.7 \times 10^5$).

Theoretical predictions of the noise reductions using the theory of Howe (1991b) were in poor agreement with experimental data. Contrary to theory, serrations with larger wavelength to amplitude ratio, λ/h, were found to achieve higher attenuation levels.

As stated earlier, the experimental investigation detailed in this paper is part of an ongoing study on the noise reduction potential of trailing edge serrations. The next stage of this study involves analysing the directivity characteristics of the trailing edge noise and taking detailed measurements of the flow field about the trailing edge region with hot-wire anemometry to gain insight into the serration noise reduction mechanism. This will in turn assist in maximising the reduction capability of trailing edge serrations and aid development of quiet airfoil technology.

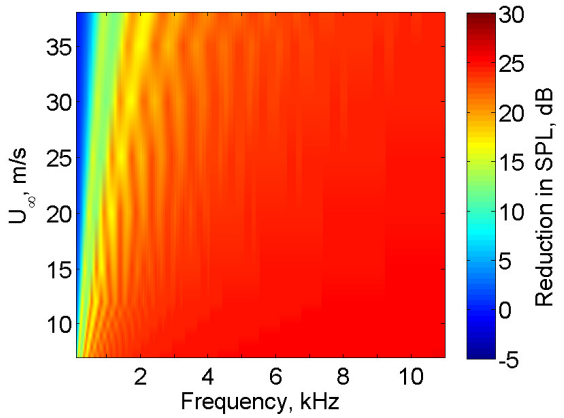

(a) Narrow serrations with λ = 3 mm.

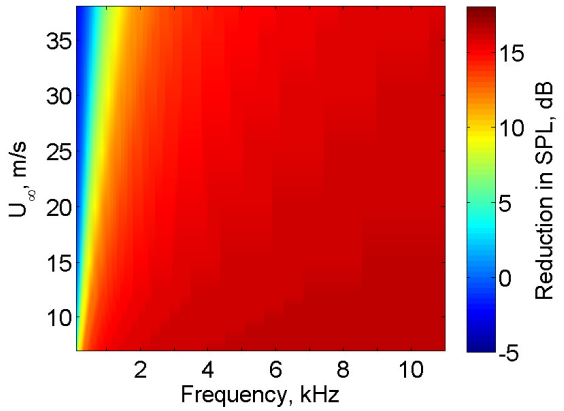

(b) Wide serrations with λ = 9 mm.

Figure 10. Noise reduction for sawtooth serrations predicted with the theory of Howe (1991b) at U_∞ = 7 – 38 m/s. Note the differing colorbar scales.

ACKNOWLEDGEMENTS

This work has been supported by the Australian Research Council under grant DP1094015 'The mechanics of quiet airfoils'.

REFERENCES

Blake, WK 1986, *Mechanics of Flow Induced Sound and Vibration*, vol. I and II, Academic Press, London, UK.

Braun, KA, Van der Borg, NJCM, Dassen, AGM, Doorenspleet, F, Gordner, A, Ocker, J and Parchen, R 1999, 'Serrated trailing edge noise (S*TENO)', *Proceedings of the European Wind Energy Conference*, Nice, France, 1-5 March.

Cebeci, T and Bradshaw, P 1977, *Momentum transfer in boundary layers*, Hemisphere Publishing Corp, Washington DC.

Chong, TP, Joseph, P, and Gruber, M 2010, 'An experimental study of airfoil instability noise with trailing edge serrations', *Proceedings of the 16th AIAA/CEAS Aeroacoustics Conference*, Stockholm, Sweden, 7 - 9 June.

Chong, TP, Joseph, P, and Gruber, M 2011 'On the noise and wake flow of an airfoil with broken and serrated trailing

edges', *Proceedings of the 17th AIAA/CEAS Aeroacoustics Conference*, Portland, Oregon, 5 - 8 June.

Dassen, T, Parchen, R, Bruggeman, J, and Hagg, F, 1996, 'Results of a wind tunnel study on the reduction of airfoil self-noise by the application of serrated blade trailing edges', *Proceedings of the European Union Wind Energy Conference and Exhibition*, Gothenburg, Sweden, 20 - 24 May.

Gruber M, Joseph, P and Chong, TP 2010, 'Experimental investigation of airfoil self noise and turbulent wake reduction by the use of trailing edge serrations', *Proceedings of the 16th AIAA/CEAS Aeroacoustics Conference*, Stockholm, Sweden, 7 - 9 June.

Gruber M, Joseph, P and Chong, TP 2011, 'On the mechanisms of serrated airfoil trailing edge noise reduction', *Proceedings of the 17th AIAA/CEAS Aeroacoustics Conference*, Portland, Oregon, 5 - 8 June.

Howe, MS 1991a, 'Aerodynamic noise of a serrated trailing edge' *Journal of Fluids and Structures*, vol. 5, pp. 33–45.

Howe, MS, 1991b 'Noise produced by a sawtooth trailing edge' *Journal of the Acoustical Society of America*, vol. 90, no. 1, pp. 482–487.

Howe, MS 1998, *Acoustics of fluid-structure interactions*, Cambridge University Press, New York.

Lockard, DP and Lilley, GM 2004, 'The airframe noise reduction challenge', Technical Report NASA/TM-2004-213013, NASA.

Moreau, DJ, Doolan, CJ, Tetlow, MR, Roberts, M, and Brooks LA 2010a, 'The flow and noise generated by a sharp trailing edge', *Proceedings of the 17th Australasian Fluid Mechanics Conference*, Auckland, New Zealand, 5-9 December.

Moreau, DJ, Tetlow, MR, Brooks, LA and Doolan CJ 2010b, 'Acoustic analysis of at plate trailing edge noise', *Proceedings of the 20th International Congress on Acoustics, ICA 2010*, Sydney Australia, 23 – 27 August.

Oerlemans, S, Fisher, M, Maeder, T and Kogler, K 2009 'Reduction of wind turbine noise using optimized airfoils and trailing edge serrations', *AIAA Journal*, vol. 47, no. 6, pp.1470 - 1481.

Oerlemans, S, Schepers, JG, Guidati, G and Wagner, S 2001, 'Experimental demonstration of wind turbine noise reduction through optimized airfoil shape and trailing-edge serrations', *Proceedings of the European Wind Energy Conference*, Copenhagen, Denmark, 2 - 6 July.

Parchen, R, Hoffmans, W, Gordner, Q, Braun, KA, Van der Borg, NJCM and Dassen, AGM 1999, 'Reduction of airfoil self-noise at low Mach number with a serrated trailing edge', *Proceedings of the 6th International Congress on Sound and Vibration*, Copenhagen, Denmark, 5 - 8 July.